Silica nanospheres for filtering higher-order optical fiber modes

Guigen Liu,[1,2] Yihui Wu,[1,*] Kaiwei Li,[1,2] Peng Hao,[1] and Ming Xuan[1]

[1]State Key Laboratory of Applied Optics, Changchun Institute of Optics, Fine Mechanics and Physics, Chinese Academy of Sciences, Changchun 130033, China

[2]University of Chinese Academy of Sciences, Beijing 100039, China

*Corresponding author: yihuiwu@ciomp.ac.cn

Received 7 November 2012; revised 3 January 2013; accepted 3 January 2013; posted 4 January 2013 (Doc. ID 179473); published 30 January 2013

Tapered optical fibers (TOFs) modified by 400 nm-diameter silica nanospheres have been experimentally and theoretically investigated. Responses of the modified TOFs (MTOFs) to methylene blue (MB) solution and surrounding refractive index (RI) have been compared. The higher-order modes are effectively filtered by the silica nanospheres, which is visualized by the interferometric output spectrum of the MTOF. The higher-order mode filtering makes the MTOF respond to MB solution with reduced sensitivity, which endows the MTOF with the potential for distinguishing the RI property from the absorption property of the molecules under detection. © 2013 Optical Society of America

OCIS codes: 060.2310, 060.2370, 290.4020, 290.5825.

1. Introduction

During the last decade, the study of fiber-optic sensors based on nanoparticles has been a domain of great interest due to special optical effects on a nanoscale [1–5], such as localized surface plasma resonance and scattering effects. Cheng and Chau [1] proposed a biochemical sensor on the basis of modification of the unclad portion of an optical fiber with self-assembled gold colloids. This proof-of-concept kind of sensor responds linearly to the surrounding refractive index (RI), showing great promise in label-free detection of molecular or biomolecular binding at the surface of gold particles. Corres *et al.* [2] devised a nanostructured fiber-optic probe for humidity sensing. This humidity sensor consists of a standard single-mode-fiber pigtail coated with a multilayer film of SiO_2 nanospheres on the tip surface, which is characterized by a very low recovery time. Monzón-Hernández *et al.* [4] showed that optical microfibers decorated with PdAu nanoparticles can serve as hydrogen sensors with fast response.

In a previous work from our group [6], a tapered optical fiber (TOF) refractometer was enhanced by modifying the waist region with a coating of SiO_2 nanospheres. The combination of nanosphere-induced scattering losses and multimode propagation of the tapered fiber gave rise to a broadened detection range and improved sensitivity for RI sensing. However, in contrast to the enhanced RI sensing, further experiments showed unexpectedly that this modified TOF (MTOF) was less sensitive to the absorption of surrounding medium than the original TOF without nanospheres. Furthermore, the spectral output of the MTOF showed regular oscillation compared to the irregular spectrum of the TOF. These phenomena were attributed to the higher-order-mode filtering by the silica nanospheres, which might provide an alternative to the other mode filter techniques, such as nonadiabatic fiber tapers [7–9]. Thus, the aim of this paper is the experimental and theoretical investigation of these phenomena induced by the nanoscale modulation of light and discuss the potential applications.

1559-128X/13/040775-05$15.00/0

2. Experiments

The experimental setup shown in Fig. 1 includes a white LED as the light source, a lens for collimating the light to illuminate the input end face of the TOF, and a spectrometer for recording the transmitted spectrum. A section of optical fiber (SMF-28, Corning) is stripped of coating and fixed in a silicon chamber that serves as both etching and sample cell. The silicon chamber is manufactured through micro-electronic-mechanical-system fabrication technology [10].

Monodispersed silica nanospheres were synthesized according to the Stöber process [11] with slight modification. The nanospheres are immobilized on the surface of the smooth TOFs through covalent attachment [12]. In addition to silica nanospheres, other dielectric nanospheres, such as polystyrene nanospheres, have similar scattering properties and may also be used. Figures 2(a) and 2(b) show the waist of the TOF and MTOF, respectively. Before modification, the waist is rather smooth, the transmitted light in the TOF is perfectly confined within the core, and no power escapes, as shown by the long-time exposure micrograph [Fig. 2(c)]. After

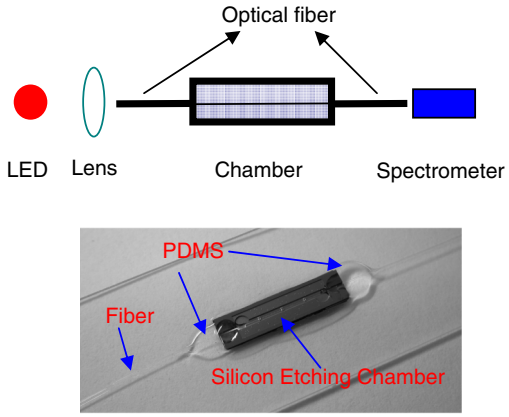

Fig. 1. (Color online) Experimental setup. The top schematic shows the configuration and the bottom image illustrates the detailed structure of the silicon chamber supporting the TOF.

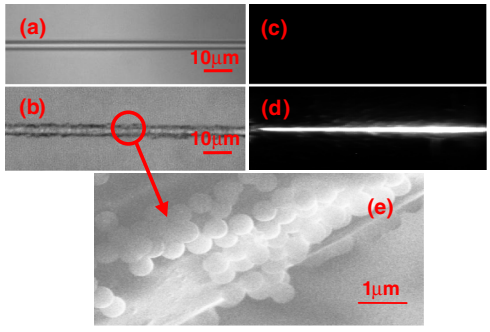

Fig. 2. (Color online) Optical microscope images of the waist of (a) TOF and (b) MTOF. Long-time exposure micrographs of the waist of (c) TOF and (d) MTOF guiding wide-bandwidth light. (e) Close view of the immobilization of 400 nm-diameter silica nanospheres onto the fiber surface.

modification, the waist surface becomes very rough, the guided light through the MTOF is strongly scattered by the nanospheres and leaks from the fiber core, as shown by Fig. 2(d). The scanning electron microscope image [Fig. 2(e)] shows that the 400 nm-diameter silica nanospheres are firmly immobilized onto the fiber surface, but they are not so uniformly distributed.

In Fig. 3(a), the normalized transmission spectrum of a 3 μm-thick TOF immersed in pure water was first measured. It can be seen that the spectrum of the TOF in water varies irregularly as wavelength changes. Subsequently, the TOF was modified by 400 nm-diameter silica nanospheres. The spectral response of the MTOF shows pronounced oscillation over a broad wavelength range of 500–700 nm. The periodicity increases slightly as wavelength increases. Figure 3(b) plots the measured output spectrum of a 5 μm-thick TOF as a function of the wavelength at different refractive indices. When the surrounding RI increases from 1.348 to 1.453, the variation in spectrum becomes more and more regular. Figure 3(c) shows the spectral responses of a TOF with varying waist diameter surrounded by water. The spectrum shows regular oscillation when the waist diameter is reduced to 1.2 μm.

The absorbance sensitivities of the TOF and MTOF were also measured. The absorbance of TOF to methylene blue (MB) solutions was first measured, followed by the modification of TOF by silica nanospheres and then the absorbance measurements of the MTOF. The absorbancy of TOF and MTOF as a function of the MB concentration is plotted in Fig. 3(d). The slope of the linear fitting line for TOF is 0.176 compared to 0.022 for MTOF, i.e., a large portion (~88%, in this case) of the sensitivity is reduced by introducing 400 nm-diameter silica nanospheres to the fiber surface. However, this experiment is not optimized because the RI and the size of the nanospheres and the parameters of tapered fiber will affect the extent of sensitivity reduction.

3. Theoretical Calculation and Analysis

Theoretical analysis is provided to investigate the experiments, in which a white LED is collimated by a lens to normally illuminate the input end face of the sensing fiber. When the illumination is added without tilt, the fundamental HE_{11} mode is largely excited, but the excitation efficiencies of other higher-order modes are very low [13]. For the sake of simplicity, only the power in HE_{11} mode excited by the LED is theoretically considered to reveal the underlying mechanism. The TOF has abrupt transition regions, therefore, mode coupling occurs when the fundamental HE_{11} mode goes through the nonadiabatic taper region. Actually, the coupling only occurs between modes having the same azimuthal eigen number, i.e., HE_{11} mode will only get coupled into HE_{1m} and HE_{1m} modes [13,14]. In particular, coupling mainly occurs between HE_{11} and

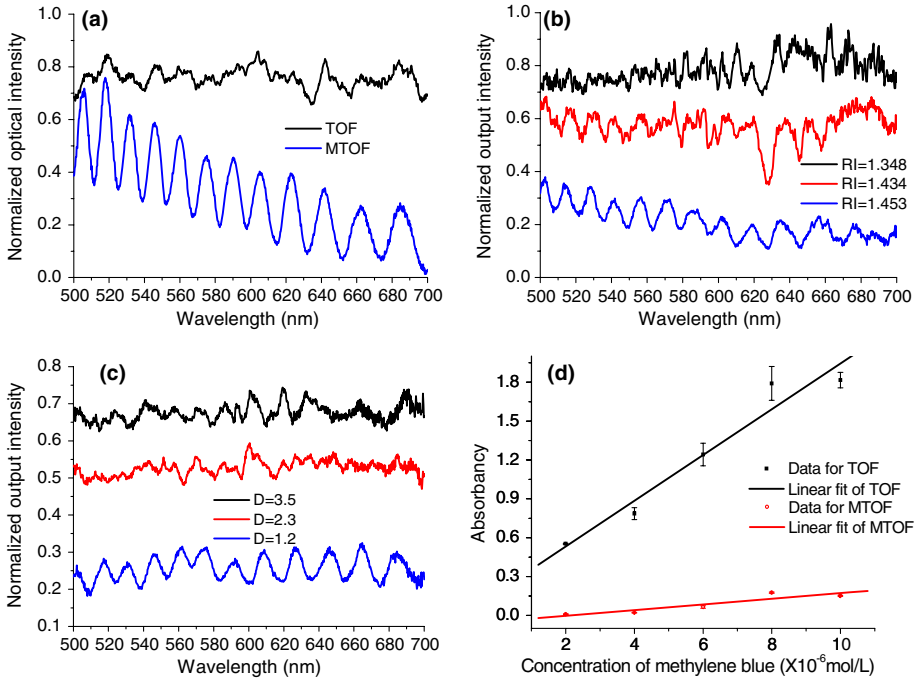

Fig. 3. (Color online) Normalized spectral responses of (a) TOF and MTOF with a 3 μm-thick waist immersed in water, (b) a TOF with a 5 μm-thick waist immersed in glycerin aqueous solutions with different refractive indices, and (c) a TOF with varying waist diameter immersed in water. D, waist diameter; unit, μm. (d) Absorbancy of TOF and MTOF with respect to the MB concentration.

HE_{12} modes whose propagation constants are the closest. A stepwise model [15] can be used to evaluate the abrupt taper, as shown in Fig. 4(a). A fraction of the power of HE_{11} mode in the input section transfers to HE_{1m} and EH_{1m} modes in the waist and then they mainly couple back into HE_{11} mode in the output section. The calculated power of various modes excited in the waist section is shown in Fig. 4(b). Calculation parameters are core RI $n_1 = 1.462$, cladding RI $n_2 = 1.457$, and external medium RI $n_e = 1.333$. The input, waist, and output sections have core radii of 4.1, 1.5 and 4.1 μm, respectively, and the operating wavelength is 633 nm. Clearly, most of the power is transferred to HE_{11} and HE_{12} modes in the waist section, especially when the waist diameter is close to the original fiber core. For instance, over 90% of power is coupled into HE_{11} and HE_{12} modes when the waist diameter exceeds 6 μm.

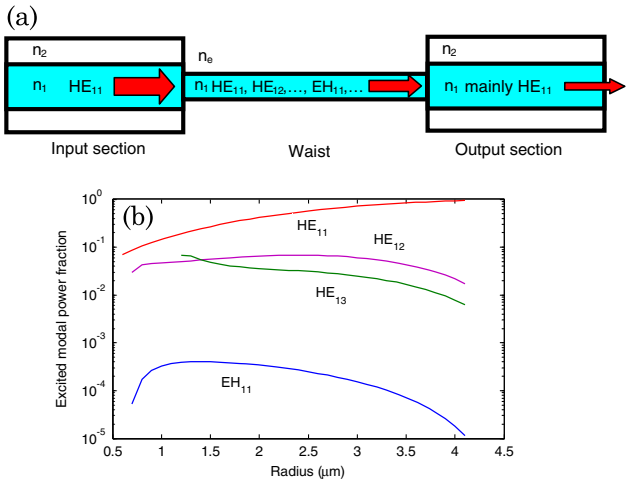

Fig. 4. (Color online) (a) Stepwise model showing the mode coupling for abrupt tapers. (b) Excited modal power fraction in the waist by the HE_{11} mode from the input section with respect to waist radius.

When silica nanospheres are immobilized onto the waist surface, the evanescent field is scattered, and some power is lost. The process of scattering losses is similar to the absorbance of an optical-fiber absorbing sensor [6], i.e., scattering and absorbance have the same effect because they both cause power loss through the attenuation of the evanescent wave. Therefore, the remaining power of a certain mode propagating through the waist region of the MTOF can be modeled according to the absorbing fiber-optic sensor as follows [6,10]:

$$P_{Rj} = P_{Sj} \exp(-\eta_j Q_{\text{sca}} N), \tag{1}$$

where P_{Rj}, P_{Sj}, and η_j are the remaining power, starting power, and power fraction in the evanescent field of the jth mode in the waist section, respectively; and Q_{sca} and$N$ are scattering efficiency and number of silica nanospheres, respectively. The scattering efficiency Q_{sca}, which is the ratio of scattering cross section and geometrical cross section, is calculated according to the Mie theory [16]. The silica nanosphere has a RI of 1.475 [17].

In Eq. (1), the interference between nanospheres and the coupling effect between modes are neglected for simplicity, and the total scattering loss is a linear

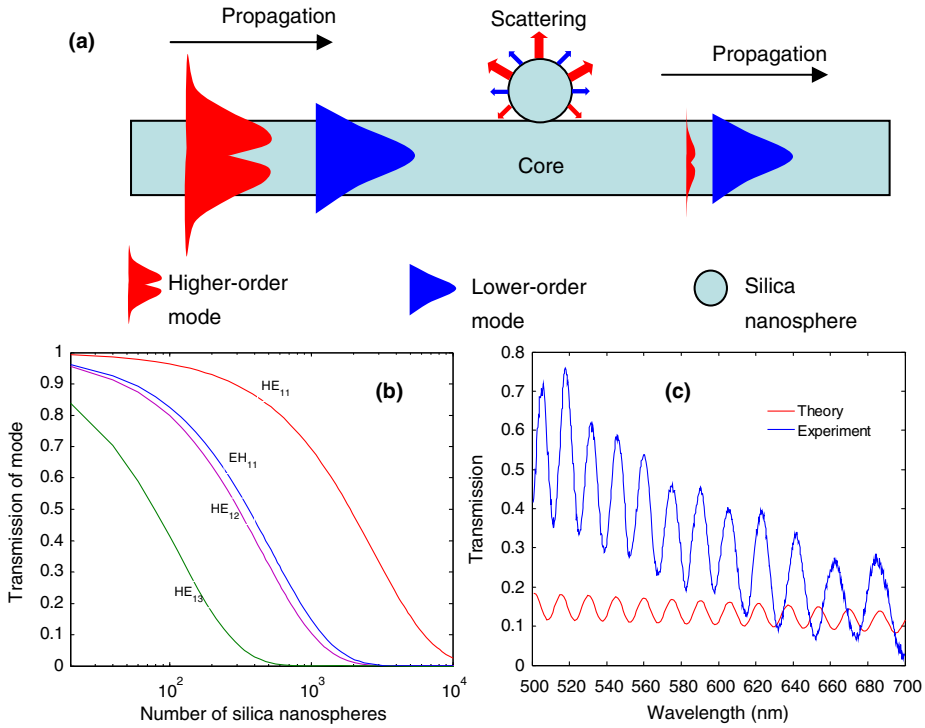

Fig. 5. (Color online) (a) Schematic representing the scattering of modes by a silica nanosphere. (b) Calculated transmission (P_{Rj}/P_{Sj}) of mode as a function of the number of silica nanospheres. (c) Calculated (bottom red curve) oscillatory spectral response due to beating between HE_{11} and HE_{12} modes, and the experimental result (top blue curve) shown in Fig. 3(a) is plotted again for comparison.

summation of all nanospheres. From Fig. 2(e), most of the nanospheres are directly attached to the fiber surface, i.e., they are equally exposed to the evanescent field. Thus, it is reasonable to assume that all the nanospheres equivalently scatter the evanescent power regardless of their specific position on the fiber surface.

Each optical-fiber bound mode has a fraction of power propagating in the evanescent field. For a given fiber, higher-order modes have larger power fractions in the evanescent field. Thus, the higher-order modes are more severely scattered by silica nanospheres on the fiber surface than the lower-order modes are, as schematically shown in Fig. 5(a). As quantitatively illustrated in Fig. 5(b), the fundamental HE_{11} mode is much less attenuated by the silica nanospheres than higher-order modes of HE_{12}, HE_{13}, and EH_{11}. For instance, only one percent of power survives for the HE_{13} mode when the number of silica nanospheres reaches 520, in which case the remaining power percentages of HE_{11}, HE_{12}, and EH_{11} are 82, 31, and 37, respectively. Although EH_{11} mode has slightly smaller attenuation than HE_{12}, it is much less excited [circa 2 orders of magnitude less, as shown in Fig. 4(b)], and the power transmitted through the EH_{11} mode is negligible. As a result, the waist works mainly with two modes: HE_{11} and HE_{12}. The two-mode operation results in a pronounced interferometric behavior in the output spectrum, as experimentally presented by the blue curve in Fig. 3(a) and theoretically shown in Fig. 5(c). This interferometric behavior is further proven by the beating spectrum seen with a TOF whose waist is surrounded by a high RI of 1.453 [see Fig. 3(b)] or has a small diameter of 1.2 μm [Fig. 3(c)]. In fact, a waist surrounded by high RI or having a small diameter has a small fiber parameter $V = 2\pi a(n_1^2 - n_2^2)^{1/2}/\lambda$, where a, n_1, n_2 and λ are radius, core RI, surrounding RI, and wavelength, respectively. The HE_{12} and HE_{13} modes have a cut-off $V = 3.832$ and 7.016, respectively, thus, the blue curves in Fig. 3(b) ($V = 5.089 \sim 3.635$ when $\lambda = 500 \sim 700$ nm) and 3(c) ($V = 4.527 \sim 3.773$ when $\lambda = 500 \sim 700$ nm) are the results of beating between HE_{11} and HE_{12} modes (HE_{13} and other higher-order modes are cut off). However, the more obvious and regular oscillation in the spectrum of MTOF [the blue curve in Fig. 3(a)] over the TOF with the low fiber parameter [blue curves in Figs. 3(b) and 3(c)] indicates that the silica nanosphere is an efficient tool for filtering higher-order modes. As the number of nanospheres exceeds 2080, the residual power in HE_{12} and other higher-order modes is less than one percent, which suggests the single-mode (HE_{11}) operation is possible. However, this single-mode operation is at the price of attenuation of more than 53% of the power in HE_{11} mode, and it is difficult to exactly control the number of nanospheres at the present time.

The discrepancy between the experimental and calculated spectra in Fig. 5(c) may be due to the simplifications in the theoretical model. Neglect of other higher-order modes except HE_{11} and HE_{12} could

make the overall calculated power lower than the experimental output. Coupling between modes due to the nonuniform coating of nanospheres would contribute to a stronger power exchange between HE_{11} and HE_{12} and thus larger oscillatory amplitude in the experimental spectrum. The slight difference in periodicity between the experiments and theory may be attributed to the simplifications in modeling the TOF [6,13]. Despite these discrepancies, the theory qualitatively reflects the experiments and well explains the phenomenon of filtering higher-order modes by silica nanospheres.

Owing to the higher-order mode filtering, the small remaining cladding power fraction of lower-order modes gives rise to the great sensitivity drop for MTOF as illustrated in Fig. 3(d). As a result, while silica nanospheres help increase the sensitivity of a TOF when used for RI detection [6], they make the TOF more immune to the absorbing surrounding medium. In some practical situations, such as measuring the RI of biomolecules, this MTOF may be a promising tool to extract the RI information with little interference from the absorbance properties of the biomolecules.

4. Conclusions

In conclusion, when silica nanospheres are immobilized onto the surface of a TOF, higher-order modes are severely scattered and effectively stripped off, resulting in the interferometric output spectrum of the MTOF. The mode-filtering effect is verified by the oscillatory transmission spectrum obtained from a TOF with a low V number. In addition, the great reduction in absorbancy sensitivity after nanosphere modification is a result of higher-order-mode filtering, which may find applications in extracting the RI information from some absorbing biomolecules with reduced interference from the absorbance properties. However, this MTOF is inappropriate for a detecting medium based on an absorbance assay.

The work is supported by the National High Technology Research and Development Program (No. 2012AA040503), National Natural Science Foundation (No. 60971025), National Key Foundation (No. 11034007), and Natural Science for Youth Foundation (No. 61102023) of China.

References

1. S.-F. Cheng and L.-K. Chau, "Colloidal gold-modified optical fiber for chemical and biochemical sensing," Anal. Chem. **75**, 16–21 (2003).
2. J. M. Corres, I. R. Matias, M. Hernaez, J. Bravo, and F. J. Arregui, "Optical fiber humidity sensors using nanostructured coatings of SiO_2 nanoparticles," IEEE Sens. J. **8**, 281–285 (2008).
3. S. Korposh, S. W. James, S.-W. Lee, S. Topliss, S. C. Cheung, W. J. Batty, and R. P. Tatam, "Fiber optic long period grating sensors with a nanoassembled mesoporous film of SiO_2 nanoparticles," Opt. Express **18**, 13227 –13238 (2010).
4. D. Monzón-Hernández, D. Luna-Moreno, D. M. Escobar, and J. Villatoro, "Optical microfibers decorated with PdAu nanoparticles for fast hydrogen sensing," Sens. Actuators B **151**, 219–222 (2010).
5. Y.-H. Su, Y.-F. Ke, S.-L. Cai, and Q.-Y. Yao, "Surface plasmon resonance of layer-by-layer gold nanoparticles induced photoelectric current in environmentally-friendly plasmon-sensitized solar cell," Light Sci. Appl. **1**, e14 (2012).
6. G. Liu, Y. Wu, K. Li, P. Hao, P. Zhang, and M. Xuan, "Mie scattering-enhanced fiber-optic refractometer," IEEE Photonics Technol. Lett. **24**, 658–660 (2012).
7. D. Donlagic, "In-line higher order mode filters based on long highly uniform fiber tapers," J. Lightwave Technol. **24**, 3532–3539 (2006).
8. Y. Jung, G. Brambilla, and D. J. Richardson, "Broadband single-mode operation of standard optical fibers by using a sub-wavelength optical wire filter," Opt. Express **16**, 14661–14667 (2008).
9. S. Moon and D. Y. Kim, "Effective single-mode transmission at wavelengths shorter than the cutoff wavelength of an optical fiber," IEEE Photonics Technol. Lett. **17**, 2604–2606 (2005).
10. Y. Wu, X. Deng, F. Li, and X. Zhuang, "Less-mode optic fiber evanescent wave absorbing sensor: parameter design for high sensitivity liquid detection," Sens. Actuators B **122**, 127–133 (2007).
11. W. Stöber and A. Fink, "Controlled growth of monodisperse silica spheres in the micron size range," J. Colloid Interface Sci. **26**, 62–69 (1968).
12. T. Cass and F. S. Ligler, *Immobilized Biomolecules in Analysis: A Practical Approach* (Oxford University, 1999).
13. A. W. Snyder and J. D. Love, *Optical Waveguide Theory*, (Chapman & Hall, 1983).
14. P. M. Shankar, L. C. Bobb, and H. D. Krumboltz, "Coupling of modes in bent biconically tapered single-mode fibers," J. Lightwave Technol. **9**, 832–837 (1991).
15. S. Lacroix, R. Bourbonnais, F. Gonthier, and J. Bures, "Tapered monomode optical fibers: understanding large power transfer," Appl. Opt. **25**, 4421–4425 (1986).
16. C. F. Bohren and D. R. Huffman, *Absorption and Scattering of Light by Small Particles* (Wiley, 1983).
17. B. N. Khlebtsov, V. A. Khanadeev, and N. G. Khlebtsov, "Determination of the size, concentration, and refractive index of silica nanoparticles from turbidity spectra," Langmuir **24**, 8964–8970 (2008).